The Astrophysical Journal, 698:1767–1770, 2009 June 20 doi:10.1088/0004-637X/698/2/1767

THE DUSTY NUCLEAR TORUS IN NGC 4151: CONSTRAINTS FROM GEMINI NEAR-INFRARED INTEGRAL FIELD SPECTROGRAPH OBSERVATIONS

Rogemar A. Riffel[1], Thaisa Storchi-Bergmann[1], and Peter J. McGregor[2]
[1] Universidade Federal do Rio Grande do Sul, IF, CP 15051, Porto Alegre 91501-970, RS, Brazil; rogemar@ufrgs.br
[2] Research School of Astronomy and Astrophysics, Australian National University, Cotter Road, Weston Creek, ACT 2611, Australia
Received 2009 February 13; accepted 2009 March 19; published 2009 June 4

ABSTRACT

We have used a near-infrared (near-IR) nuclear spectrum (covering the Z, J, H, and K bands) of the nucleus of NGC 4151 obtained with the Gemini Near-Infrared Integral Field Spectrograph (NIFS) and adaptive optics, to isolate and constrain the properties of a near-IR unresolved nuclear source whose spectral signature is clearly present in our data. The near-IR spectrum was combined with an optical spectrum obtained with the Space Telescope Imaging Spectrograph which was used to constrain the contribution of a power-law component. After subtraction of the power-law component, the near-IR continuum is well fitted by a blackbody function, with $T = 1285 \pm 50$ K, which dominates the nuclear spectrum—within an aperture of radius 0.″3—in the near-IR. We attribute the blackbody component to emission by a dusty structure, with hot dust mass $M_{\rm HD} = (6.9 \pm 1.5) \times 10^{-4}\ M_{\odot}$, not resolved by our observations, which provide only an upper limit for its distance from the nucleus of 4 pc. If the reddening derived for the narrow-line region also applies to the near-IR source, we obtain a temperature $T = 1360 \pm 50$ K and a mass $M_{\rm HD} = (3.1 \pm 0.7) \times 10^{-4}\ M_{\odot}$ for the hot dust. This structure may be the inner wall of the dusty torus postulated by the unified model or the inner part of a dusty wind originating in the accretion disk.

Key words: galaxies: active – galaxies: individual (NGC 4151) – galaxies: ISM – galaxies: nuclei

1. INTRODUCTION

The presence of a very compact infrared source in the nucleus of the Seyfert galaxy NGC 4151 was first suggested by the observations of Penston et al. (1974), who reported photometric variations of the galaxy nucleus both in the optical and in the near-infrared (hereafter near-IR). A close inspection of the light curves shown by Penston et al. (1974) suggests a delay between the near-IR and optical variations, recently confirmed by Minezaki et al. (2004), who could better quantify its value as 48^{+2}_{-3} days. These authors concluded that the K-band emission is dominated by thermal radiation from hot dust located at ≈0.04 pc from the nucleus. A similar interpretation was previously proposed by Rieke & Lebofsky (1981), via models fitted to a large aperture (∼8″) nuclear optical and near-IR spectrum, concluding that in the near-IR the emission is dominated by thermal reradiation by hot dust with temperature $T_{\rm HD} = 1300$–1500 K.

Mundell et al. (2003) have reported neutral hydrogen absorption in VLA radio observations with subparsec linear resolution, close to the systemic velocity of the galaxy, interpreted as due to a clumpy gas layer suggested to be associated with a circumnuclear obscuring torus. According to Mundell et al. (2003), this absorption is observed along the line of sight toward the first component of the radio counterjet, at ⩽0.1 pc from the nucleus, thus consistent with the estimated inner radius of ≈0.04 pc derived by Minezaki et al. (2004). The interpretation put forth by Mundell et al. (2003)—that the obscuring torus is not in front of the active galactic nucleus (AGN)—is necessary in order to reconcile the radio observations with the UV/optical observations which show a blue nuclear continuum and broad emission lines, indicating that both the nuclear source and the broad-line region are visible.

The presence of a dusty torus around the nucleus of NGC 4151 was disputed by Swain et al. (2003) on the basis of interferometric observations at 2.2 μm using the two 10 m Keck telescopes. These authors found a marginally resolved nuclear source ⩽0.1 pc in diameter—consistent with the observations of both Mundell et al. (2003) and Minezaki et al. (2004), but favor an origin for this emission in thermal gas from the accretion disk, arguing that previous nuclear spectra of NGC 4151 did not show an "infrared bump," in apparent contradiction with the previous study by Rieke & Lebofsky (1981). Such a bump is expected if a dusty torus is present, due to reprocessing of UV/optical radiation from the central engine (e.g., Rieke & Lebofsky 1981; Barvainis 1987; Sanders et al. 1989).

The alternative interpretation proposed by Swain et al. (2003) seems nevertheless to be in line with recent results presented by Kraemer et al. (2008), who studied the distribution of [O III] λ5007 and [O II] λ3727 emission in the narrow-line region (NLR) of NGC 4151. These authors pointed out that there does not seem to be a region of complete shadow around the apex of the bicone, as significant ionized gas emission is found there, although with a lower ionization parameter, consistent with a weaker ionizing flux. Kraemer et al. (2008) propose that the attenuation of the nuclear radiation could be due to low-ionization absorbers swept out by a wind originating in the accretion disk, suggesting that there is no need for a "classical, doughnut-shaped" torus in order to explain the observed light distributions, in agreement with recent modeling for the obscuring region around an AGN (Elitzur 2008).

In this work, we present new observations of the nucleus of NGC 4151 with the Gemini Near-Infrared Integral Field Spectrograph (NIFS) at an angular resolution of 0.″12—corresponding to a spatial resolution of a few parsecs at the galaxy—which is much improved relative to previous spectroscopic studies. Our observations clearly reveal the presence of an unresolved nuclear source in the near-IR. We have already used the NIFS data to map the excitation (Storchi-Bergmann et al. 2009, hereafter Paper I) and kinematics (R. Simões Lopes et al. 2009, in preparation) of the NLR. In the present paper, we use the nuclear spectrum, combined with surrounding

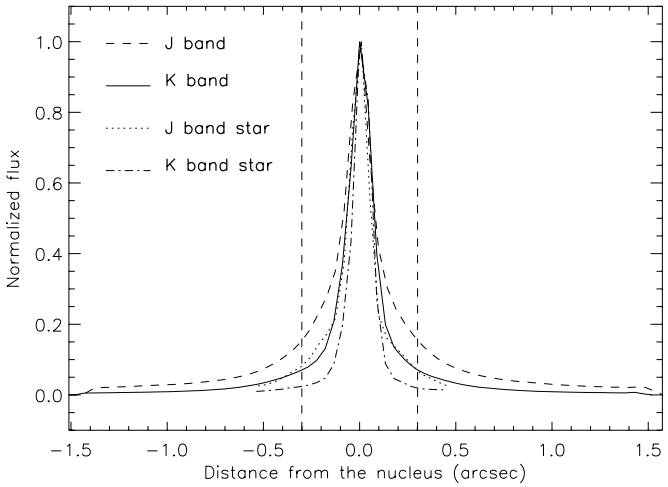

Figure 1. Spatial profiles for the galaxy and of a star at the *J* and *K* bands. The vertical dashed lines mark the extraction aperture of the nuclear spectrum (0.″3 radius).

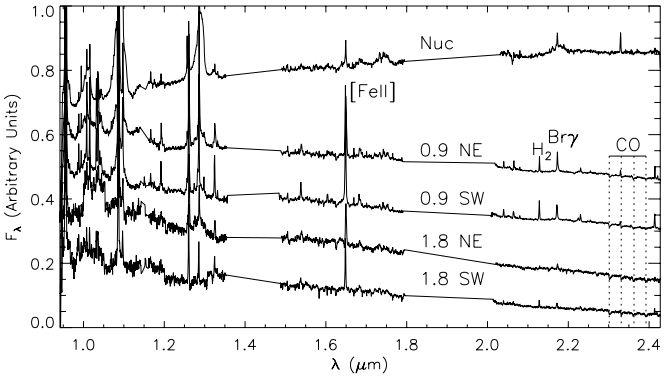

Figure 2. Nuclear spectrum (top) obtained for a circular aperture with 0.″3 radius and extranuclear spectra at the positions 0.″9 NE, 0.″9 SW, 1.″8 NE, and 1.″8 SW, normalized to the flux at the nucleus at $\lambda \approx 1$ μm. The spectra are shown in arbitrary flux units and are shifted by a constant for clarity.

extranuclear spectra and a Space Telescope Imaging Spectrograph (STIS) optical spectrum, in order to isolate the emission of the infrared nuclear source, which is consistent with that predicted for the torus postulated in the unified model of AGNs (Antonucci 1993).

We adopt a distance to NGC 4151 of 13.3 Mpc, corresponding to a scale at the galaxy of 65 pc arcsec^{-1} (Mundell et al. 2003). This paper is organized as follows. In Section 2, we present a summary of the observations; in Section 3, we present the results; and in Section 4, we present and discuss our conclusions.

2. OBSERVATIONS

Two-dimensional spectroscopic data were obtained on the Gemini North telescope with the instrument NIFS (McGregor et al. 2003) operating with the adaptive optics module ALTAIR on the nights of 2006 December 12 and 13. The observations covered the spectral bands *Z*, *J*, *H*, and *K*, at spectral resolutions of 4990, 6040, 5290, and 5290, respectively, resulting in a wavelength coverage from 0.94 μm to 2.40 μm. More details of the observations and reduction procedures can be found in Storchi-Bergmann et al. (2009).

In the present paper, we concentrate on the analysis of the nuclear continuum. The spatial profiles of the nuclear region of the galaxy in the *K* and *J* bands are shown in Figure 1, in comparison with stellar profiles. The nuclear source—which has a full width at half-maximum (FWHM) of 0.″12 ± 0.″02 in the *K* band and 0.″16 ± 0.″02 in the *J* band—corresponding to 8.0 ± 1.3 pc and 10.4 ± 1.3 pc at the galaxy, respectively—is unresolved by our observations, in spite of the fact that their spatial profiles are marginally broader than those of the stars in Figure 1. As discussed in Storchi-Bergmann et al. (2009), this is due to the much shorter exposures of the stellar observations.

In order to include as much as possible of the nuclear source, we have chosen an extraction aperture of 0.″3 radius which includes the nuclear flux down to 10% of the peak value in the *K* band, as illustrated by the dashed lines in Figure 1.

3. RESULTS

The nuclear spectrum is shown in Figure 2, together with extranuclear spectra obtained through similar 0.″3 apertures at distances of 0.″9 NE, 0.″9 SW, 1.″8 NE, and 1.″8 SW from the nucleus, normalized to the flux of the nuclear spectrum at $\lambda \approx 1$ μm. Fluxes of more than 50 emission lines have been measured and listed in Table 1 of Paper I for the nuclear and two extranuclear spectra.

From Figure 2, as well as from spectra shown in Paper I, we observe that the extranuclear spectra are blue at all locations around the nucleus. As this blue continuum is observed up to at least 2 arcsec from the nucleus, it cannot be due to the AGN and can thus be attributed to a young stellar population surrounding the nucleus. Absorption features from stellar CO bands are indeed observed in the *K* band, marked by the vertical dotted lines in Figure 2. Only right at the nucleus the continuum is clearly very red. Similar red nuclear continua have been observed for other AGNs and attributed to emission from hot dust, possibly from a dusty torus around the supermassive black hole, with temperature close to the dust sublimation temperature (Barvainis 1987; Marco & Alloin 1998, 2000; Rodríguez-Ardila et al. 2005b; Rodríguez-Ardila & Mazzalay 2006; Riffel et al. 2009).

3.1. Nuclear Optical Continuum

In order to better constrain the nuclear spectral energy distribution (SED), we have used an optical STIS spectrum of the nucleus extracted within a similar aperture to that of our near-IR spectrum, obtained from the atlas of AGN spectra compiled by Spinelli et al. (2006). This spectrum was extracted within an aperture of 0.″2 × 0.″1 and covers the spectral range 0.3–1 μm. We have used the continuum region from 9780 to 9820 Å to normalize the optical spectrum to the same flux as our near-IR spectrum (which extends down to the *Z* band) as there is a flux difference of ≈30% between the STIS spectrum and our nuclear spectrum. The small difference between the apertures is not important because the stellar contribution, when compared with the nuclear one, is small, as discussed below. We show the optical plus near-IR spectrum in Figure 3. The optical continuum is very blue and can be well reproduced by a power law up to ≈1 μm, where there is a change in slope and a red component begins to appear in the near-IR. Although the near-IR emission is dominated by this component, the contribution of the power law in the near-IR is not negligible in the *Z*, *J*, and *H* bands, as discussed below.

3.2. Modeling the Spectral Energy Distribution

We have modeled the optical+near-IR nuclear continuum of NGC 4151 by the sum of two components: a power law, which

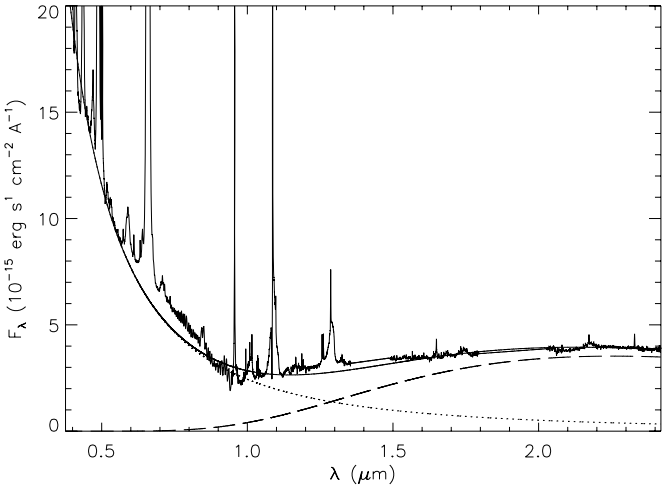

Figure 3. Optical+near-IR nuclear spectrum of NGC 4151 together with a fit (continuous line) considering the contribution of a power law (dotted line) plus a blackbody function (dashed line).

seems to dominate in the optical, plus a blackbody function, which dominates in the near-IR, as illustrated in Figure 3. The fit was performed using the *nfit1d* task from the STSDAS IRAF package, which allows the selection of limited spectral intervals for the fit. We have excluded the spectral interval between 0.6 and 0.9 μm from the fit as we have estimated that the contribution of the Paschen continuum in this interval ($\approx 1.3 \times 10^{-15}$ erg cm^{-2} s^{-1} A^{-1} at 8200 Å) is not negligible when compared with the total flux observed in the continuum. Moreover, the quality of the optical spectrum in its red end is quite poor, and should not be used to constrain the SED. Excluding the above spectral region, the best fit was obtained for a power law $F_\lambda \propto \lambda^{-2.25}$ and a blackbody function of temperature $T = 1285 \pm 50$ K, which peaks at $\approx$2.3 μm. The fit of the two functions combined is shown in Figure 3 as a continuous line, while the blackbody component is shown as a dashed line and the power law as a dotted line.

We have next evaluated the effect of the underlying stellar population in the fit above. A stellar population spectrum was extracted from our near-IR data cubes within a ring around the nucleus with an inner radius of 0.″6 and an outer radius of 0.″9. We have then normalized the flux of this extranuclear spectrum to 15% of the peak nuclear flux in the *K* band, which is the maximum contribution of the stellar population estimated from a spatial profile through the nucleus. Under the assumption that the underlying stellar population in the nuclear spectrum is the same as that from the ring (which is supported by other spectra from the nuclear vicinity), we have then subtracted the extranuclear spectrum from the nuclear one. As we do not have an extranuclear optical spectrum, we repeated the fit for the near-IR only, comparing the temperature of the uncorrected to the corrected spectrum, concluding that, within the uncertainties ($\approx$50 K), the blackbody temperature is the same.

The reddening may also affect the results of the fit. An estimate of the reddening in the near-IR can be obtained from the emission lines of the NLR. We have used the [Fe II]λ1.2570 μm/λ1.6440 μm line ratio to calculate the reddening (as described in Paper I, but using the present nuclear spectrum, for an aperture of radius 0.″3), resulting in $E(B-V) \approx 0.6$. It is not clear that this reddening applies to the optical continuum. If it does, it would result in a very steep power law for the corrected nuclear continuum: using the extinction curve of Rieke & Lebofsky (1985), we obtain $F_\lambda \propto \lambda^{-4.5}$. Nevertheless, the presence of broad lines in the spectra and the already very blue continuum suggests that the reddening of the optical spectrum is much smaller; we may be seeing the nuclear source through a low-extinction window to the nucleus. This may also apply to the near-IR nuclear source, but, even if the extinction applies, the correction in the near-IR is small. A reddening correction of only the near-IR spectrum for $E(B-V) = 0.6$, keeping the power-law index the same, results in a revised blackbody temperature of $T = 1360 \pm 50$ K.

Table 1
Masses of Hot Dust Found in AGNs

Galaxy	$M_{\rm HD}$ ($M_\odot$)	Reference
NGC 4151	6.9×10^{-4}	This work (no extinction, see the text)
NGC 7582	2.8×10^{-3}	Riffel et al. (2009)
Mrk 1239	2.7×10^{-2}	Rodríguez-Ardila & Mazzalay (2006)
Mrk 766	2.1×10^{-3}	Rodríguez-Ardila et al. (2005b)
NGC 1068	1.1×10^{-3}	Marco & Alloin (2000)
NGC 7469	5.2×10^{-2}	Marco & Alloin (1998)
NGC 4593	5.0×10^{-4}	Santos-Lléo et al. (1995)
NGC 3783	2.5×10^{-3}	Glass (1992)
NGC 1566	7.0×10^{-4}	Baribaud et al. (1992)
Fairall 9	2.0×10^{-2}	Clavel et al. (1989)

3.3. The Hot Dust Mass

Following Barvainis (1987) and Riffel et al. (2009), we can estimate the mass of the hot dust producing the unresolved near-IR emission. First, we obtain the infrared spectral luminosity of each dust grain, in erg s^{-1} Hz^{-1}, assuming that the dust is composed of graphite grains, by

$$L^{\rm gr}_{\nu,{\rm ir}} = 4\pi^2 a^2 Q_\nu B_\nu(T_{\rm gr}), \quad (1)$$

where a is the grain radius, Q_ν is the absorption efficiency, and $B_\nu(T_{\rm gr})$ is its spectral distribution assumed to be a Planck function with temperature $T_{\rm gr}$.

The number of dust grains ($N_{\rm HD}$) can be estimated from the ratio between the total luminosity of the hot dust $\left(L^{\rm HD}_{\rm ir}\right)$ and the total luminosity of one dust grain $\left(L^{\rm gr}_{\rm ir}\right)$ as $N_{\rm HD} = \frac{L^{\rm HD}_{\rm ir}}{L^{\rm gr}_{\rm ir}}$. $L^{\rm HD}_{\rm ir}$ was obtained by integrating the flux under the Planck function fitted to the nuclear spectrum and adopting a distance to NGC 4151 of $d = 13.3$ Mpc, while $L^{\rm gr}_{\rm ir}$ was obtained by the integration of Equation (1) for a temperature of $T_{\rm gr} = 1285$ K. Finally, the mass of the emitting hot dust is obtained by

$$M_{\rm HD} \approx \frac{4\pi}{3} a^3 N_{\rm HD} \rho_{\rm gr}. \quad (2)$$

Assuming a graphite density of $\rho_{\rm gr} = 2.26$ g cm^{-3} (Granato & Danese 1994), we obtain $M_{\rm HD} = (6.9 \pm 1.5) \times 10^{-4}\ M_\odot$.

If we assume that the near-IR nuclear source is subject to reddening, we should then use the temperature $T_{\rm gr} = 1360$ K, which will lead to a smaller dust mass of $M_{\rm HD} = (3.1 \pm 0.7) \times 10^{-4}\ M_\odot$.

In Table 1, we present a comparison of the mass of hot dust obtained here for NGC 4151 with those derived for other AGNs in previous works. This comparison reveals that the hot dust mass for NGC 4151 is similar to those obtained for NGC 1068 by Marco & Alloin (2000), for NGC 4593 by Santos-Lléo et al. (1995), and for NGC 1566 by Baribaud et al. (1992)

and is smaller than the masses derived for other galaxies such as NGC 7582, Mrk 1239, Mrk 766, NGC 7469, NGC 3783, and Fairall 9 by Riffel et al. (2009), Rodríguez-Ardila & Mazzalay (2006), Rodríguez-Ardila et al. (2005b), Marco & Alloin (1998), Glass (1992), and Clavel et al. (1989), respectively.

4. DISCUSSION AND CONCLUSIONS

As discussed in Section 1, Swain et al. (2003) observed NGC 4151 at 2.2 μm and have marginally resolved a nuclear source $\leqslant$0.1 pc in diameter, concluding that the emission was due to thermal gas from the central accretion disk instead of a dusty torus, as they claimed that previous observations did not show the bump. Our near-IR nuclear spectrum (Figure 2) clearly shows this bump and favors emission by hot dust as the dominant mechanism for its origin, in agreement with previous studies using larger aperture data (Rieke & Lebofsky 1981). A more recent near-IR spectrum obtained by Riffel et al. (2006), although with lower spatial resolution than ours, also suggests the presence of the bump.

The modern view of the torus (Elitzur 2008) is not of a static doughnut shape structure but of a clumpy wind of dusty and optically thick clouds originating in the black hole accretion disk, a view which has recently been favored also in the case of NGC 4151 by Kraemer et al. (2008), and which is in partial agreement with the proposition by Swain et al. (2003). Being clumpy, the dusty wind allows the view of the nuclear source through low-extinction holes. The presence of such holes is also supported by the observation of ionized gas close to the apex of the bicone, beyond its presumed walls. This more updated view is also consistent with our data and results from previous papers discussed above, if we consider that the near-IR nuclear source can be identified with the hottest part of the dusty wind, which is the one closest to the nucleus and which emits most of the near-IR radiation. According to our data, the temperature of this dust is $T = 1285 \pm 50$ K and its mass is $M_{\rm HD} = (6.9 \pm 1.5) \times 10^{-4}\ M_{\odot}$, obtained by fitting the optical and near-IR spectrum. The observation of the nuclear continuum and of the broad emission lines suggest that we are looking to the nuclear source through a low-extinction window, in spite of the fact that the estimated reddening from the emission lines of the NLR is $E(B-V) = 0.6$. If we assume that this reddening is also affecting the nuclear source, we obtain $T = 1360 \pm 50$ K for the dust temperature and mass $M_{\rm HD} = (3.1 \pm 0.7) \times 10^{-4}\ M_{\odot}$. The temperatures obtained are in good agreement with those previously obtained by Rieke & Lebofsky (1981). Comparison between our near-IR flux values with theirs shows that the nucleus was 3–4 times brighter than in the epoch of our observations, suggesting that the temperature of the hot dust does not depend on the AGN luminosity.

Regarding the location of the hot dust, our spatial resolution allows us to put only an upper limit to the radius of the infrared source of 4 pc (half the FWHM of the nuclear source). Similar scales have been probed by Storchi-Bergmann et al. (2005), who found a heavily obscured starburst closer than 9 pc from the nucleus in NGC 1097 and argued that it could be located in the outskirts of the torus. Jaffe et al. (2004) using mid-IR interferometric observations constrained the dust emission in NGC 1068 to originate in a region of only 1 pc diameter. In the case of NGC 4151, optical and near-IR monitoring observations of Minezaki et al. (2004) provide a better constraint on the location of the inner radius of the torus at $\approx$0.04 pc from the nucleus.

The NLR of NGC 4151 has an approximate biconical morphology with a projected opening angle of $\sim$75° and with its axis oriented along a P.A. $\sim$60/240° (NE–SW). The SW side of the bicone is tilted toward us, making an angle of 45° with the line of sight, according to Das et al. (2005), who also gives an opening angle of the cone of 66°, which puts our line of sight just outside the cone wall. If the torus is oriented perpendicularly to the cone, we are looking down into the torus hole. This allows us to constrain the half-height of the torus to less than 0.04 pc for a "doughnut shape" opaque torus. This torus should extend to at least 0.1 pc from the nucleus, in order to contain the neutral hydrogen clouds observed by Mundell et al. (2003). As proposed by these authors, the NE part of the radio jet would be behind the torus, while the SW part would be in front of it.

We thank the referee Dr. George Rieke for valuable suggestions which helped to improve the present paper. This work is based on observations obtained at the Gemini Observatory, which is operated by the Association of Universities for Research in Astronomy, Inc., under a cooperative agreement with the NSF on behalf of the Gemini partnership: the National Science Foundation (United States), the Science and Technology Facilities Council (UK), the National Research Council (Canada), CONICYT (Chile), the Australian Research Council (Australia), Ministrio da Cincia e Tecnologia (Brazil), and Ministerio de Ciencia, Tecnologa e Innovacin Productiva (Argentina). This work has been partially supported by the Brazilian institution CNPq and Australian Research Council.

REFERENCES

Antonucci, R. 1993, ARA&A, 31, 473
Baribaud, T., Alloin, D., Glass, I., & Pelat, D. 1992, A&A, 256, 375
Barvainis, R. 1987, ApJ, 320, 537
Clavel, J., Wamsteker, W., & Glass, I. S. 1989, ApJ, 337, 236
Das, V., et al. 2005, AJ, 130, 945
Elitzur, M. 2008, New Astron. Rev., 52, 274
Glass, I. 1992, MNRAS, 256, 23P
Granato, G. L., & Danese, L. 1994, MNRAS, 268, 235
Jaffe, W., et al. 2004, Nature, 429, 47J
Kraemer, S. B., Schmitt, H. R., & Crenshaw, D. M. 2008, ApJ, 679, 1128
Marco, O., & Alloin, D. 1998, A&A, 336, 823
Marco, O., & Alloin, D. 2000, A&A, 353, 465
McGregor, P. J., et al. 2003, in Proc. SPIE Vol. 4841, Instrument Design and Performance for Optical/Infrared Ground-based Telescopes, ed. M. Iye, & A. F. M. Moorwood (Bellingham, WA: SPIE), 1581
Minezaki, T., Yoshii, Y., Kabayashi, Y., Enya, K., Suganuma, M., Tomita, H., Aoki, T., & Peterson, B. 2004, AJ, 600, L35
Mundell, C. G., Wrobel, J. M., Pedlar, A., & Gallimore, J. 2003, ApJ, 583, 192
Penston, M. V., Penston, M. F., Selmes, R. A., Becklin, E. E., & Neugebauer, G. 1974, MNRAS, 169, 357
Rieke, G. H., & Lebofsky, M. J. 1981, ApJ, 250, 87
Rieke, G. H., & Lebofsky, M. J. 1985, ApJ, 288, 618
Riffel, R., Rodríguez-Ardila, A., & Pastoriza, M. G. 2006, A&A, 457, 61
Riffel, R. A., Storchi-Bergmann, T., Dors, Jr., O. L., & Winge, C. 2009, MNRAS, 393, 783
Rodríguez-Ardila, A., Contini, M., & Viegas, S. 2005b, MNRAS, 357, 220
Rodríguez-Ardila, A., & Mazzalay, X. 2006, MNRAS, 367, L57
Sanders, D. B., Phinney, E. S., Neugebauer, G., Soifer, B. T., & Matthews, K. 1989, ApJ, 347, 29
Santos-Lléo, M., Clavel, J., Barr, P., Glass, I. S., Pelat, D., Peterson, B. M., & Reichert, G. 1995, MNRAS, 274, 1
Spinelli, P. F., Storchi-Bergmann, T., Brandt, C. H., & Calzetti, D. 2006, ApJS, 166, 498
Storchi-Bergmann, T., Mc Gregor, P. J., Riffel, R. A., Simões Lopes, R., Beck, T., & Dopita, M. 2009, MNRAS, in press (arXiv:0812.2448v1)
Storchi-Bergmann, T., Nemmen, R. S., Spinelli, P. F., Eracleous, M., Wilson, A. S., Filippenko, A. V., & Livio, M. 2005, ApJ, 624, 13
Swain, M., et al. 2003, ApJ, 596, L166